Near-field diffractive elements

Daniel Marks

The Beckman Institute for Advanced Science and Technology, University of Illinois at Urbana–Champaign, Urbana, Illinois 61801

P. Scott Carney

Department of Electrical and Computer Engineering and The Beckman Institute for Advanced Science and Technology, University of Illinois at Urbana–Champaign, Urbana, Illinois 61801

Received December 14, 2004

A novel near-field imaging system is proposed and simulated. It is seen that a significant improvement in performance in the presence of noise is possible without loss of resolution. © 2005 Optical Society of America

OCIS codes: 180.5810, 050.1970.

Near-field optics[1–3] has brought the resolution achievable with optical imaging in the visible and near-visible range of the spectrum to size scales approaching that of tens of atoms, orders of magnitude smaller than the wavelength and so well below the optical resolution limits of Abbe[4] and Rayleigh.[5] The benefits inherent in ultramicroscopic imaging capabilities affect a broad array of fields in research, medicine, and manufacturing.

The essential idea in modern near-field scanning optical microscopy (NSOM) may be traced to Synge.[6] Synge proposed that the Abbe–Rayleigh resolution limits might be overcome by illuminating the thin sample through a small hole in a black screen in the near zone of the sample. By recording the throughput as a function of position of the small hole, an image is obtained with resolution on the scale of the aperture size rather than the wavelength. Decades after the inital proposal, Synge's vision was realized using a metal-coated fiber with a small aperture formed at the end playing the role of the screen. Also in practice today is a method in which no aperture is formed in the fiber tip. In that method, the apertureless case, the near field is coupled to the far zone by diffraction from a sharp metallic tip. The superresolution achievable in scanning probe modalities is attributable to the conversion of high-spatial-frequency waves, i.e., evanescent waves, into propagating modes of the field either in free space or in the fiber. This conversion takes place by diffraction from the subwavelength aperture of the probe. The subwavelength structure of the object is related to these high-spatial-frequency components of the field.[7–11]

The various forms of scanning microscopy in use today suffer from common problems of image acquisition speed and photon inefficiency. A scanned tip inherently operates in serial fashion. In this work, the theory of near-field diffractive elements that offer the opportunity to register data in a parallel fashion is investigated. It is suggested that the probe tip be replaced by a near-field diffractive element (NDE) that scatters the high-spatial-frequency components of the field into propagating modes. As an example, a Fresnel lens scanned in the near zone of a sample is considered. It will be seen that this scheme may be made highly photon efficient, as opposed to scanning probe methods.

A scalar field model is considered at fixed frequency $\omega_0 = k_0 c$. The sample is described by a complex susceptibility $\eta(\mathbf{r})$, and the NDE is described by the susceptibilty $\chi(\mathbf{r})$. The field obeys the equation $\nabla^2 U(\mathbf{r}) + k_0^2 U(\mathbf{r}) = -4\pi k_0^2 [\eta(\mathbf{r}) + \chi(\mathbf{r})] U(\mathbf{r})$. It is assumed that the sample is illuminated by a unit amplitude plane wave $U_i(\mathbf{r}) = \exp(i\mathbf{k}_i \cdot \mathbf{r})$, where $\mathbf{k}_i \cdot \mathbf{k}_i = k_0^2$. The field scattered to the far zone may be calculated to first order in both the NDE and the sample susceptibilities. It is assumed that the background terms corresponding to scattering from only the NDE and only the sample may be subtracted by performing the scattering experiment with only those elements present. The terms corresponding to scattering of the incident field first from the NDE and then the sample are neglected, which yields a good approximation especially if the incident field is evanescent. The field thus coupled out of the instrument and assumed to be measured holographically, U_m, is given by the expression

$$U_m(\mathbf{r}) = k_0^4 \int \mathrm{d}^3 r' \int \mathrm{d}^3 r'' U_i(\mathbf{r}'') \eta(\mathbf{r}'') \times G(\mathbf{r}', \mathbf{r}'') \chi(\mathbf{r}') G(\mathbf{r}, \mathbf{r}'), \quad (1)$$

where $G(\mathbf{r}, \mathbf{r}')$ is the Green function. It is assumed that the sample and the NDE are uniform over the thickness of the sample and NDE, respectively (see Fig. 1); samples with a nontrivial three-dimensional structure will be addressed in another work. For simplicity, $G(\mathbf{r}, \mathbf{r}')$ is taken to be the free-space Green function $G(\mathbf{r}, \mathbf{r}') = \exp(ik_0|\mathbf{r} - \mathbf{r}'|)/|\mathbf{r} - \mathbf{r}'|$. Substrate boundaries may be included by modification of this Green function.[12] The NDE may be translated laterally over the sample by a displacement $\mathbf{r}_0$ (see Fig. 1). This field is measured holographically in the far zone of the sample and NDE at position $\mathbf{r} = r\hat{r}$ by means of a conventional far-field optical system so that the

0146-9592/05/141870-3/$15.00

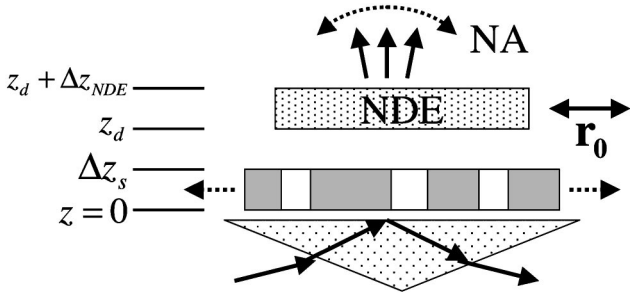

Fig. 1. Arrangement of the NDE imaging system.

resultant measured field is given by the expression

$$U_m(\mathbf{r},\mathbf{r}_0) \sim \frac{k_0^4 \exp(ik_0 r)}{2\pi r} \int \mathrm{d}^2 q\, \tilde{\chi}(\mathbf{q}) \exp(i\mathbf{q}\cdot\mathbf{r}_0) \times M(\mathbf{q},\mathbf{r})\tilde{\eta}(\mathbf{q} - k_0\hat{r}_\parallel - \mathbf{q}_i), \tag{2}$$

where $\hat{r}_\parallel$ is the vector projection of the unit vector $\hat{r}$ into the plane of the sample. Here M is given by the expression

$$M(\mathbf{q},\mathbf{r}) = i \times \frac{\exp\{-i[k_0 z/r - k_z(\mathbf{q} - k_0\hat{r}_\parallel)]z_d\}(\exp\{-i[k_0 z/r - k_z(\mathbf{q} - k_0\hat{r}_\parallel)]\Delta z_{NDE}\} - 1)(1 - \exp\{-i[k_z(\mathbf{q} - k_0\hat{r}_\parallel) - k_z(\mathbf{q})]\Delta z_s\})}{k_z(\mathbf{q} - k_0\hat{r}_\parallel)[k_z(\mathbf{q} - k_0\hat{r}_\parallel) - k_z(\mathbf{q})][k_0 z/r - k_z(\mathbf{q} - k_0\hat{r}_\parallel)]}, \tag{3}$$

and $k_z(\mathbf{q}) = \sqrt{k_0^2 - q^2}$.

If the NDE is scanned over a large area compared with the sample, then the Fourier transform of the resultant data set with respect to the NDE translation yields a relatively simple relationship between the data and the Fourier components of the sample:

$$\tilde{U}_m(\mathbf{r},\mathbf{Q}) = \frac{k_0^4 \exp(ik_0 r)}{r} M(\mathbf{Q},\mathbf{r})\tilde{\chi}(\mathbf{Q})\tilde{\eta}(\mathbf{Q} - k_0\hat{r}_\parallel - \mathbf{q}_i). \tag{4}$$

Equation (4) may be written in terms of an integral operator K such that $\tilde{U}_m = K\eta$. An approximate reconstruction η^+ of η may thus be obtained from the data by the formula $\eta^+ = [K^* K]^+ K^* U_m$, where K^* is the Hermitian adjoint of K and $[K^*K]^+$ is the pseudoinverse of the normal operator $[K^*K]$. The pseudoinverse $[K^*K]^+$ is the inverse of $[K^*K]$ restricted to the orthogonal complement of the null space of the operator. To assess the resolution of such a system, it is useful to compute $[K^*K]$, which may be seen to have kernel $[K^*K](\mathbf{Q}\mathbf{Q}')$ given by the expression

$$[K^*K](\mathbf{Q}',\mathbf{Q}) = \delta(\mathbf{Q}' - \mathbf{Q}) \int_S \mathrm{d}^2\hat{r}_\parallel |M(\mathbf{Q}' + k_0\hat{r}_\parallel + \mathbf{q}_i, \mathbf{r})\tilde{\chi}(\mathbf{Q}' + k_0\hat{r}_\parallel + \mathbf{q}_i)|^2, \tag{5}$$

where the range of integration, S, is determined by the numerical aperture (NA) of the far-zone imaging system used to measure the field, S being the disk with radius $|\hat{r}_\parallel| = \mathrm{NA}$. Note that the normal operator $K^*K(\mathbf{Q},\mathbf{Q}')$ is diagonal in the Fourier basis and will thus be written as $K^*K(\mathbf{Q})$; it is a linear space-invariant convolution even though the diffractive is not necessarily space invariant. Because $K^*K(\mathbf{Q})$ is a convolution of positive functions, the width of the bandpass must be wider than either the diffractive or free-space propagation bandpass alone and is approximately the sum of the two widths. The effect of increasing the NA is to enlarge the region S and therefore widen the bandpass already provided by the diffractive.

In principle, the bandpass of the system is given by the bandpass of $[K^*K]^+[K^*K]$, which is simply zero in the range where $[K^*K](\mathbf{Q})$ is zero and unity elsewhere.

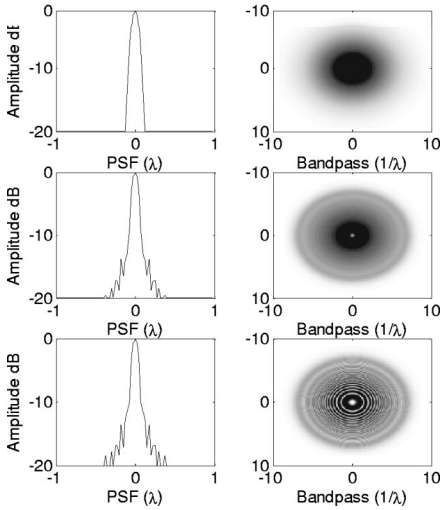

Fig. 2. Left, simulated PSF for three NDE systems, normalized to peak height. Right, normal operator for three simulations as a function of spatial frequency; a darker gray level indicates a proportionally larger bandpass weight. The top row is a simulation of a NSOM NDE with an effective radius of $\lambda/16$ and a NA of the far-field system of 0.5. The middle row is a simulation of a Fresnel plate NDE of 8λ diameter with a spatial frequency from zero at the center to $8\lambda^{-1}$ at the perimeter, with NA = 0.5. The bottom row is also a simulation of the Fresnel NDE but with NA = 0.05.

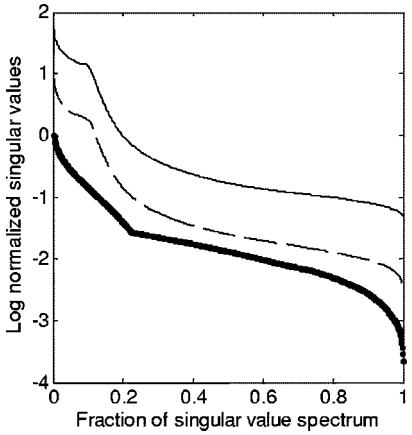

Fig. 3. Singular value spectrum of three simulated imaging systems, normalized to the highest singular value of the NSOM case. The heavy solid curve is the standard NSOM singular value spectrum. The dashed curve is the Fresnel NDE case with NA=0.05, and the thin solid curve is the Fresnel NDE case with NA = 0.5.

where. In the presence of noise, inversion of Eq. (4) must include some form of regularization to produce a meaningful, stable result. Under Tikhonov regularization with the regularization constant γ, the bandpass of the recovered point spread function is similarly space invariant, being $K^*K(\mathbf{Q})/[K^*K(\mathbf{Q})+\gamma]$.

To explore the behavior of a near-field diffractive optical system, three NDE imaging systems are considered. A near-field diffractive imaging system consisting of an amplitude Fresnel plate diffractive is simulated for two different NAs, as well as a standard pointlike diffractive element such as that used in NSOM or photon scanning tunneling microscopy. The resolution of the systems is evaluated by numerically computing the normal operator of Eq. (5). For a fair comparison, the two systems have approximately the same bandpass limit and the same value of χ_0. The object is modeled to be uniform in the depth direction and $\Delta z_s=\lambda/2$ in thickness and in near contact with the NDE at $z_d=\Delta z_s+\lambda/100$ distance. The pointlike probe is a thin disk of material with susceptibility χ_0 and diameter $\lambda/16$ to model the effective aperture of a metal-coated NSOM probe. The amplitude of the Fresnel diffractive is given by the equation

$$\chi(\mathbf{r}) = \chi_0 \cos(\pi\alpha|\mathbf{r}|^2) \text{for } |\mathbf{r}| < r_0,$$
$$\chi(\mathbf{r}) = 0 \text{ otherwise}, \quad (6)$$

with $r_0=4\lambda$ and the spatial frequency at the perimeter of the diffractive being $8\lambda^{-1}$, so that $\alpha=2\lambda^{-2}$. Thus the two NDEs exhibit comparable feature size.

The simulated bandpass and resultant point spread function of the gatof the three systems are given in Fig. 2, assuming Tikhonov regularization with a 20 dB signal-to-noise ratio. Because the Fresnel diffractive and the NSOM probe structure contain similar spatial frequencies, the limits of the bandpass are similar. When a small range of the far field is measured, there appear gaps in the bandpass function of the Fresnel NDE, as seen in the bottom plot, and sidelobes emerge in the PSF. These effects are mitigated by sampling more of the far field (corresponding to a far-field system with a larger NA) as shown in the middle plot.

The noise performance of these systems is explored by examining the spectrum of singular values of K given by the root of the eigenvalues of the normal operator, $\sqrt{K^*K(\mathbf{Q})}$, of these three cases in Fig. 3. A spectrum of larger singular values implies that the system will be more tolerant to regularization required by the presence of noise by virtue of having more singular functions above the noise floor. Generally, the singular values scale roughly as the NA of the far-zone system. It may be seen that the Fresnel diffractive with NA =0.05 exhibits a spectrum of larger singular values that the NSOM system with NA =0.5. Thus it is expected that extended NDE-based near-field imaging systems could be much more noise tolerant than pointlike NDE systems.

The singular values of the system also scale with the transverse dimensions of the NDE, roughly as the square root of the linear dimensions of the extent of the NDE. This is not surprising since a larger NDE collects more of the field scattered from the sample. NDE such as the Fresnel plate may be scaled with no loss of resolution while pointlike probes such as those used in NSOM cannot be scaled up without a corresponding loss of resolution.

In conclusion, we have proposed and simulated the behavior of a novel imaging system based on extended diffractive elements in the near zone of a sample. The signal-to-noise ratio improvement of such a system may greatly benefit near-field optical metrology when large samples with subwavelength features must be imaged. In effect, the system implements a parallel measurement of near-field features from many parts of a sample at once, increasing the throughput of the gathered signal.

This work was supported by U.S. Air Force MURI grant F49620-03-1-0379. D. Marks's e-mail address is dmarks@uiuc.edu., P. S. Carney's is carney@uiuc.edu.

References

1. D. Courjon, K. Sarayeddine, and M. Spajer, Opt. Commun. **71**, 23 (1989).
2. C. Girard and A. Dereux, Rep. Prog. Phys. **59**, 657 (1996).
3. J.-J. Greffet and R. Carminati, Prog. Surf. Sci. **56**, 133 (1997).
4. E. Abbe, Archiv. Mikroscopische Anat. **9**, 413 (1873).
5. Lord Rayleigh, Philos. Mag. **8**, 261 (1879).
6. E. Synge, Philos. Mag., **6**, 356 (1928).
7. R. A. Frazin, D. G. Fischer, and P. S. Carney, J. Opt. Soc. Am. A **21**, 1050 (2004).
8. D. G. Fischer and P. S. Carney, in *Tribute to Emil Wolf: Science and Engineering Legacy of Physical Optics* (SPIE, 2004).
9. P. S. Carney and J. C. Schotland, in *Inside Out: Inverse Problems*, G. Uhlman, ed. (Cambridge U. Press, 2003).
10. P. S. Carney and J. C. Schotland, J. Opt. A, Pure Appl. Opt. **4**, S140 (2002).
11. P. S. Carney and J. C. Schotland, Appl. Phys. Lett. **77**, 2798 (2000).
12. P. S. Carney and J. C. Schotland, J. Opt. Soc. Am. A **20**, 542 (2003).